XVI IMEKO World Congress
Measurement - Supports Science - Improves Technology - Protects Environment ... and Provides Employment - Now and in the Future
Vienna, AUSTRIA, 2000, September 25-28

EFFECTS OF MECHANICAL STRESS ON SOFT MAGNETIC MATERIALS UNDER ROTATIONAL MAGNETIZATION

C. Krell, N. Baumgartinger, E. Leiss and H. Pfützner
Inst. of Fundamentals and Theory of Electrotechnical Engineering
Bioelectricity & Magnetism Laboratory
Vienna University of Technology, Gusshausstr. 27-351, A-1040 Vienna, Austria

Abstract: This paper concerns effects of mechanical stress on soft magnetic silicon iron sheets subject to rotational magnetization (RM). RM is typical for armatures of rotating machines and for T-joint regions of transformer cores. In both cases, distinct mechanical stress may arise, e.g., from temperature changes or from clamping. Simulation of such magneto-mechanical conditions on a specifically designed test apparatus shows that tensile (or compressive) stress of several MPa intensity yields distinct effects on all three permeability, energy losses and magnetostriction.

Keywords: rotational magnetization, magnetic losses, magnetostriction, stress effects, soft magnetic materials

1 INTRODUCTION

The present study concerns effects of mechanical stress on soft magnetic silicon iron sheets subject to rotational magnetization (RM). Armatures of rotating machines and T-joint regions of transformer cores are typical areas for RM phenomena. It is well known that RM is responsible for excess no-load losses and for excess audible noise due to increased magnetostriction (MS) which stimulates worldwide research.

Additional effects arise if the considered material is under mechanical stress which may arise in practice from temperature changes or - for example - also from clamping. Stress effects have been studied in numberless works. However, almost all investigations were restricted to alternating magnetization (AM). Very few studies concern effects of stress on multidirectional magnetization processes. The present work was focused on the corresponding behavior of highly grain oriented (h.g.o.) SiFe sheets subject to RM patterns which were simulated according to practical working conditions in T-joint regions (Fig. 1).

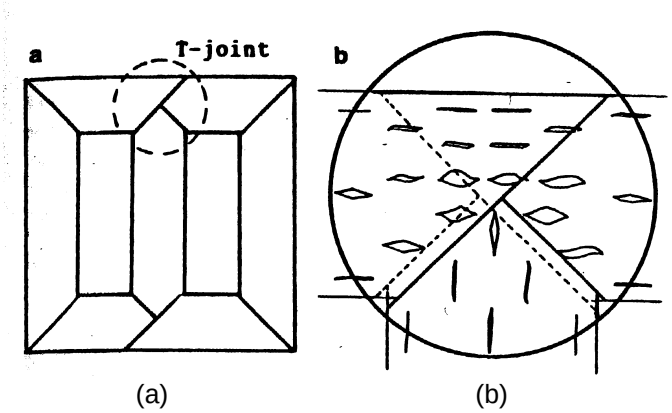

Figure 1. T-joint region of a transformer core. (a) Typical joint design.
(b) Experimentally determined time patterns of the induction vector ***B*** (after [1])

Cores of electric machines tend to show inhomogeneous stress patterns, especially compression with intensities up to several MPa. To analyze the corresponding material performance under RM, we performed well defined simulations by means of a so-called Rotational Single Sheet Tester (RSST) as closer described in [2,3]. All three, permeability, losses and MS were measured as a function of

tension and compression, respectively.

2 EXPERIMENTAL SETUP

Experiments were performed on hexagonal samples of approximately 150 mm diameter magnetized in the RSST by means of six pole pieces as shown by the photograph in Fig. 2.
Elliptical and lozenge-like ***B***-patterns were established with axial ratios

$$e = \hat{B}_{t.d.} / \hat{B}_{r.d.} \tag{1}$$

up to 0.5 in rough correspondence to practice (Fig.1b). Here, $\hat{B}_{r.d.}$ represents the maximum induction in rolling direction (r.d.) and $\hat{B}_{t.d.}$ the maximum induction in transverse direction (t.d.).

To restrict bending artifacts linked with compression, stress was established by means of a clamping device mounted on the sample by means of eight 2 mm screws. The arrangement offers approximately homogeneous stress up to about s = ±3 MPa in r.d., in the central 80 mm x 50 mm sample region.

Stress conditions were registered by means of strain gauges. The corresponding changes of ***B/H***-relations, power loss *P*, domain configurations and MS-caused strains l were determined by means of sensors which are closer described in [2,4].

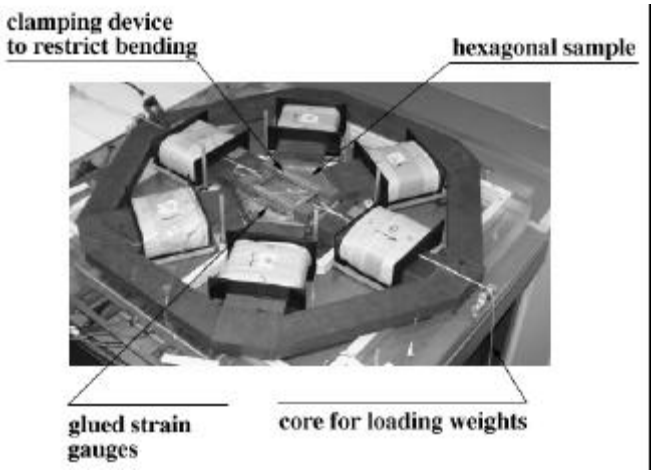

Figure 2. Experimental setup including a hexagonal sample with clamping and loading device for generation of mechanical stress.

3 DATA READOUT

3.1 Readout of the magnetic vectors ***B*** and ***H***

Fig. 3 illustrates in a schematic way the experimental establishment of data. The field vector ***H*** was determined by means of a double H-coil, the induction vector ***B*** by means of the well known needle method. Both the coils and the four needle contacts were arranged below the sample to keep the surface free for other components (clamping device and strain gauges). The four signals were fed into an oscilloscope and saved in ASCII-file format.

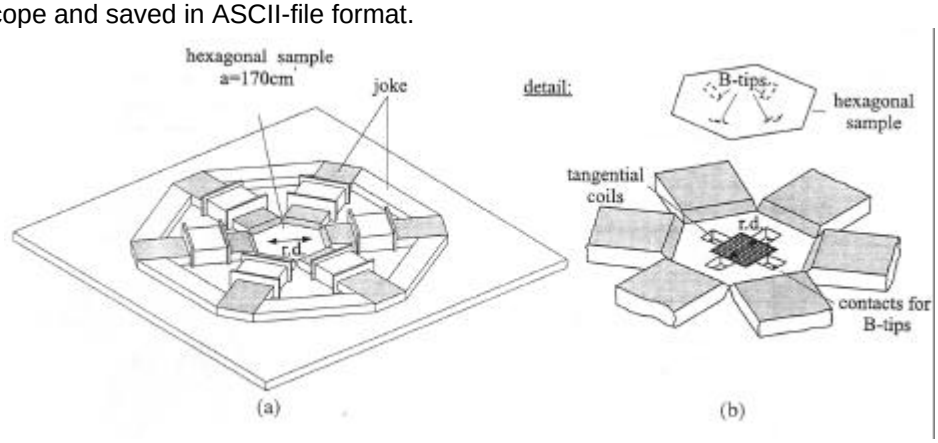

Figure 3. Schematic outline of the arrangement (a) of the sample and (b) of the components for the

detection of the vectors ***B*** and the ***H*** (see text).
The total energy loss was calculated on the basis of the Poynting vector from the components of ***B*** and ***H*** by means using the well known expression

$$P = \frac{1}{Ts}\int_0^T \left(H_{r.d.}\frac{dB_{r.d.}}{dt} + H_{t.d.}\frac{dB_{t.d.}}{dt} \right) \cdot dt \quad . \tag{2}$$

(s density of material, T the period).

3.2 Readout of the MS-caused strain l

The MS-caused strain under various stress conditions (unstressed, tension, compression) was registered by means of strain gauges of high length (50 mm) in order to average over the coarse grain structure of anisotropic types of SiFe. For the reduction of temperature artifacts, each strain gauge was complemented by a dummy gauge placed above the active one in air, both wired to a half bridge. To establish full information about the MS-caused strain patterns, measurements were taken in three directions (0°,45° and 90°) as sketched in Fig. 4.

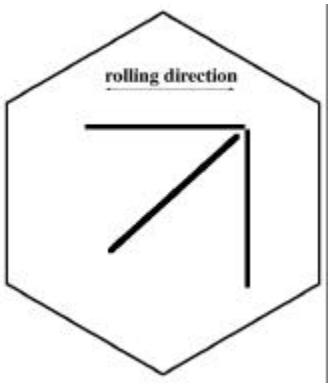

Figure 4. Arrangement of three sets of strain gauges (active gauge + dummy gauge) in the directions 0° (r.d.), 45° and 90° (t.d.).

A specific problem of measurement was caused by the very low degree of MS of modern types of SiFe. Due to modern technologies (compare, e.g., [1]), the typical order of MS for nominal magnetization in r.d. (unstressed state) is well below 1 µm/m. This yields low values of the signal-to-noise ratio as demonstrated by Fig. 5a. For the establishment of reliable data, we applied Fourier transform in order to determine the signal spectrum (Fig. 5b). In a next step, back-transformation was restricted to the most relevant spectrum lines, i.e. 100 Hz, 200 Hz and 300 Hz for magnetization with 50 Hz. Consideration of higher harmonics did not show improvements of the resulting filtered signal (Fig. 5c).

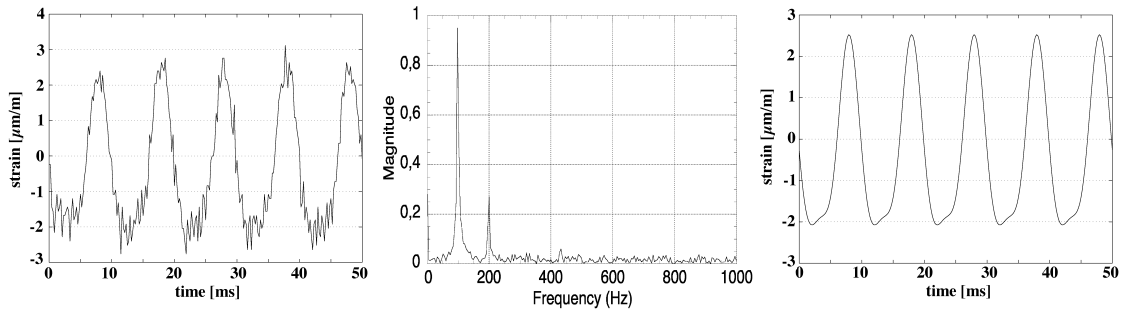

(a) (b) (c)

Figure 5. Applied procedure for filtering of MS signals (example for $B_{r.d.}$=1.6T, e = 0.5, s = -3MPa).
(a) Signal as generated by the strain gauge placed in r.d.
(b) Fourier spectrum.

(c) Result of back-transformation considering the spectral lines 100 Hz, 200 Hz and 300 Hz.

To calculate the MS-caused strain in all directions a of the sheet plane, the results $l_1(t)$, $l_2(t)$ and $l_3(t)$ of the three strain gauges were used for the establishment of the strain tensor ***s*** as closer described elsewhere [4,5]. Due to symmetry ($s_{ij} = s_{ji}$), the tensor contains only three independent quantities which can be calculated from the three measured results according to:

$$\begin{bmatrix} s_{11} \\ s_{12} \\ s_{22} \end{bmatrix} = \begin{bmatrix} \cos^2 a_1 & 2\cos a_1 \sin a_1 & \sin^2 a_1 \\ \cos^2 a_2 & 2\cos a_2 \sin a_2 & \sin^2 a_2 \\ \cos^2 a_3 & 2\cos a_3 \sin a_3 & \sin^2 a_3 \end{bmatrix}^{-1} \cdot \begin{bmatrix} l_1 \\ l_2 \\ l_3 \end{bmatrix} . \tag{3}$$

For our special case $l_1 = l(0°)$, $l_2 = l(45°)$ and $l_3 = l(90°)$ (Fig.4), we find:

$$\begin{aligned} s_{11} &= l(0°) \\ s_{12} &= -0.5 \cdot l(0°) + l(45°) - 0.5 \cdot l(90°) \\ s_{22} &= l(90°) \end{aligned} \quad . \tag{4}$$

Finally, the instantaneous MS-caused strain in an arbitrary direction a (the angle to the r.d.) results as

$$\begin{aligned} l(t,a) &= s_{11}(t) \cdot \cos^2 a + 2 s_{12}(t) \cdot \cos a \cdot \sin a + s_{22}(t) \cdot \sin^2 a = \\ &= l(t,0°) \cdot \cos a \cdot (\cos a - \sin a) + 2 l(t,45°) \cdot \cos a \cdot \sin a - l(t,90°) \cdot \sin a \cdot (\cos a - \sin a) \quad . \end{aligned} \tag{5}$$

4 RESULTS

The following figures show typical results of investigation for laser scribed, highly grain oriented SiFe (230 µm ZDKH, NSC).

4.1 Effects on the permeability

Fig. 6 shows a time pattern of the induction vector ***B*** ($B_{r.d.}$ = 1.6T; $B_{t.d.}$ = 0.8T; i.e. e = 0.5) which can be assumed to be typical for T-joint regions of transformer cores (compare Fig. 1). Fig. 6b shows the corresponding time pattern of the field vector ***H*** for all three the unstressed state, the state of tension (s = +3 MPa) and the state of compression (s = -3 MPa). Analogous to the well known case of AM, tension in r.d. resulted in a decrease of the field component in r.d. (corresponding to increased permeability in this direction) and an increase in t.d., compared to the unstressed state. Compression yielded contrary behavior. The corresponding changes were very large. For example, for the t.d., the permeability of the compressed state exceeds that of the tensile stressed state by a factor close to three. Further increases of effects can be assumed for higher levels of applied stress.

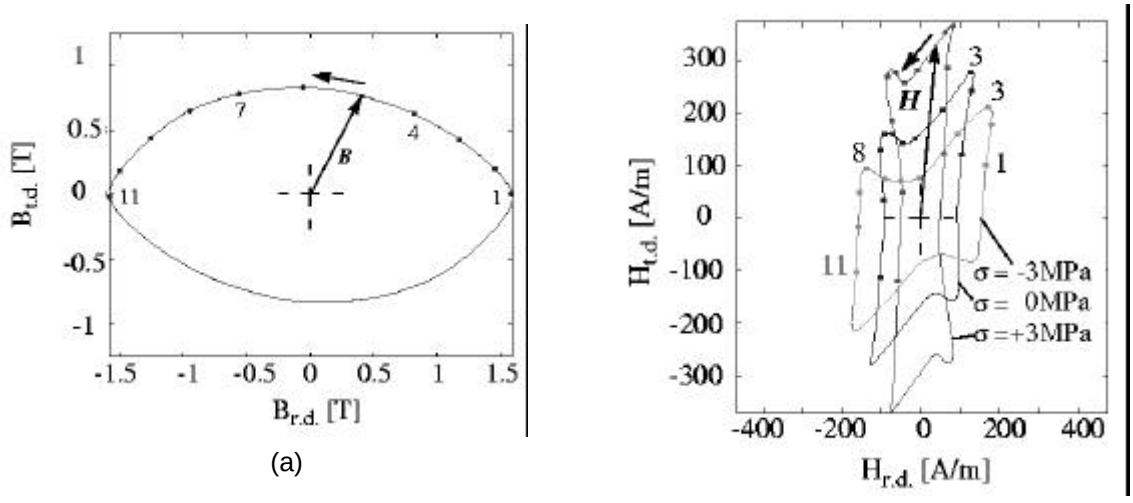

Figure 6. (a) Investigated time pattern of the induction vector ***B*** (kept constant for all stress states)
(b) corresponding time patterns of the field vector ***H*** for the unstressed state, for

compression and for tension (both in r.d.)

4.2 Effects on power losses

Fig. 7 shows "related losses"

$$p = P / P_n = P(B_{r.d.}, e, s) / P(B_{r.d.}, e = 0, s = 0) \quad (6)$$

as a function of stress. In the given case, P is the measured total loss for elliptical magnetization with $B_{r.d.}$ = 1.7 T and stress. P_n = 0.85 W/kg is the nominal loss for AM ($B_{r.d.}$ = 1.7 T, 50 Hz) without stress. According to Fig. 7a, compared to AM, RM with $e = 0.4$ yielded $r \approx 1.7$ corresponds to about 70% loss increase. Tension yielded additional 10% increase while only slight effects were observed for compression. Fig. 7b indicates that the effects of tension become much more pronounced for lower values of induction. $B_{r.d.}$ = 1.3 T yielded 120% loss increase. Finally, Fig. 7c indicates that higher values of ellipticity yield loss increases up to 300% for the unstressed state. The corresponding effects of stress will be studied in further work.

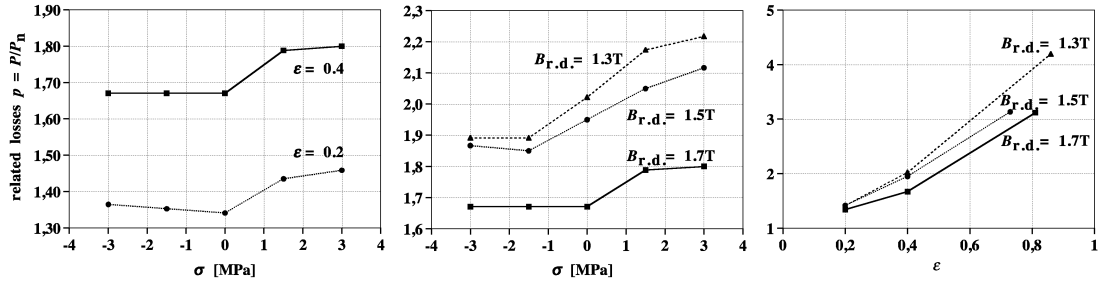

(a) (b) (c)

Figure 7. Related losses p.
(a) p as a function of stress s for two values of ellipticity e (for $B_{r.d.}$=1.7T).
(b) p as a function of stress s for e = 0.4 and three values of induction $B_{r.d.}$ in r.d.
(c) p as a function of ellipticity e for three values of $B_{r.d.}$; unstressed state (s = 0).

4.3 Effects on magnetostriction

Fig. 8 shows typical results for MS-caused strain as arising from elliptical magnetization according to Fig. 6. For example, the left graph of Fig. 8a shows the result of equation (5) for the instant of time when the vector ***B*** passes through t.d. Compared to the rotationally demagnetized state, this moment is characterized by a strong shrinkage ($l_{r.d.} \approx$ - 8 µm/m) of the r.d. compensated by a 3 µm/m elongation of the t.d. and an increase of the sheet thickness (see similar results in [2,4]).

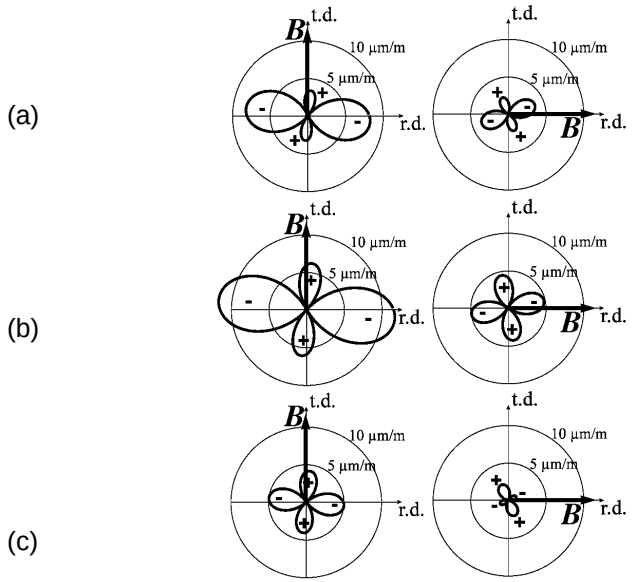

(a)

(b)

(c)

Figure 8. MS-caused strain for all directions a of the plane for the time instants of ***B*** in t.d. (left figures) and ***B*** in r.d. (right figures), respectively. Positive or negative strain values are given related to the rotationally demagnetized state.

(a) Unstressed state, (b) tension in r.d., (c) compression in r.d.

The other extreme situation arises when ***B*** passes through r.d. (right graph). The shrinkage of the r.d. is as weak as 3 μm/m in this moment which means that the peak-to-peak value $\Delta l_{\text{r.d.,max}}$ of MS-caused strain in r.d. is close to 8 - 3 = 5 μm/m.

Results for other directions or other instants of time can be evaluated in the same way. It should be stressed that all this information is offered by the signals of the three strain gauges as arising during a single period of magnetization.

Fig. 8b shows effects of tension. The moment of ***B*** in t.d. shows a very strong shrinkage in r.d. ($l_{\text{r.d}} \approx$ - 12 μm/m) which can be explained by the fact that very few magnetic spin moments are directed in t.d. in the demagnetized state. Compression (Fig. 8c) shows the contrary behavior, the t.d. being "filled up" with a considerably high amount of spins a priori. As well known, compression in r.d. enhances MS in the case of AM. On the other hand, it proves to be advantageous in the case of RM, Fig. 8c indicating a quite small value of $\Delta l_{\text{r.d.,max}}$.

As indicated by Fig. 8, MS-caused strain proves to be most pronounced in r.d. Thus, data for the latter is most relevant for industrial practice. For an effective comparison to the unstressed AM state, we suggest to offer MS-caused strain levels in a related way (as also used for loss data more above).

Fig. 9 shows data for the r.d. expressed by "related MS"

$$r_{\text{r.d.}} = \Delta l_{\text{r.d.,max}} / \Delta l_{\text{r.d.,max,n}} = \Delta l_{\text{r.d.,max}}(B_{\text{r.d.}}, e, s) / \Delta l_{\text{r.d.,max}}(B_{\text{r.d.}}, e = 0, s = 0) . \quad (7)$$

Fig. 9a shows $r_{\text{r.d.}}$ as a function of stress s for various values of ellipticity e at $B_{\text{r.d.}}$ = 1.7 T. The graph illustrates the high significance of RM, the order of $r_{\text{r.d.}}$ being as high as 30 for e = 0.4 without stress - i.e. an increase of 3000% compared to AM. Tension yielded a further increase of this ratio, compression some decrease for low loading but some increase for higher one.

Fig. 9b indicates that the effects of both RM and stress become even more pronounced for lower values of $B_{\text{r.d.}}$ the ratio $r_{\text{r.d.}}$ being up to 125 for 1.3 T. Finally, Fig.9c shows values up to $r_{\text{r.d.}} \approx$ 300 for the case of very high ellipticity $e = 0.8$, which however is not likely to arise in practice (see Fig. 1).

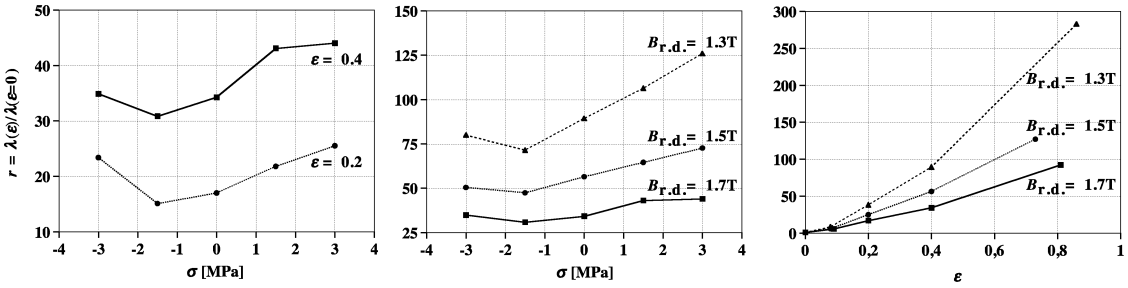

(a) (b) (c)

Figure 9. Related magnetostriction $r_{\text{r.d.}}$ in r.d.
(a) $r_{\text{r.d.}}$ as a function of stress s for two values of ellipticity e (for $B_{\text{r.d.}}$=1.7T).
(b) $r_{\text{r.d.}}$ as a function of stress s for e = 0,4 and three values of induction $B_{\text{r.d.}}$ in r.d.
(c) $r_{\text{r.d.}}$ as a function of ellipticity e at various induction in r.d., in unstressed state (s = 0).

5 CONCLUSIONS

Stress effects on the performance of highly grain oriented silicon iron under rotational magnetization (RM) were studied by means of a "rotational single sheet tester". Application of tensile or compressive stress in rolling direction (r.d.) with intensities up to 3 MPa yielded the following main results:

(1) Effects on permeability -
Various stress states affect the material permeability in different ways: Compared to the unstressed state, tension yields an increase of the permeability in r.d. and a decrease in t.d. Compression acts in a contrary way. The difference between tension and compression corresponds roughly to a factor 3 in both directions (r.d. and t.d.).

(2) Effects on losses -
Losses prove to be mainly affected by the ellipticity e. Related to AM, RM yielded loss increases up to 300 % for the unstressed state (for $B_{\text{r.d.}}$ = 1.3T, e = 0.8). In the case of tension, losses showed further increases proportional to the strength of tension, while compression lead to decreases, contrary to the well known case of AM.

(3) Effects on magnetostriction -

As in the case of losses, MS-caused strains prove to be mainly affected by the ellipticity, e.g. e = 0.2 yielding increases of more than one order of magnitude. Contrary to the well known case of AM, tension resulted in an increase of MS especially in r.d. This behavior can be explained with the fact, that tension in r.d. yields a general decrease of transverse domain fragments in favor of the r.d. Thus, the RM process involves high levels of redistribution. On the other hand, compression affects the material's performance in a less disadvantageous way.

ACKNOWLEDGEMENTS

The authors acknowledge support from the Austrian FWF (Project P10968-PHY) as well as from ABB Transformers (Ludvika, Sweden; St. Louis, USA).

REFERENCES

[1] Nippon steel corporation: Electrical steel sheets, *NSC-Catalogue* EXE367 (1984).
[2] A. Hasenzagl, H. Pfützner, A. Saito, Y. Okazaki, Status of the Vienna hexagonal single sheet tester, in: A. Kedous-Lebouc (ed.), *Proc. 5th Workshop 2D Magnetization Problems* (Grenoble, 29.-30. Sept. 1997), Laboratory of Electrotechnical Engineering Grenoble, France, 1998, 33-41.
[3] A.Hasenzagl, B.Weiser, H.Pfützner, Novel 3-phase excited single sheet tester for rotational magnetization, *J.Magn.Magn.Mater*. **160** (1996) 180-182.
[4] A.Hasenzagl, B.Weiser, H.Pfützner, Magnetostriction of 3% SiFe for 2-D magnetization patterns, *J.Magn.Magn.Mater*. **160** (1996) 55-56.
[5] W. F. Brown, *Magnetoelastic Interactions*, Springer, Berlin. 1966

AUTHORS: C. KRELL, N. BAUMGARTINGER, E. LEISS and H. PFÜTZNER; Inst. of Fundamentals and Theory of Electrotechnical Engineering, Bioelectricity & Magnetism Laboratory, University of Technology, Gusshausstr. 27-351, A-1040 Vienna, Austria
Phone Int ++43 1 58801 35110, Fax Int ++43 1 58801 35199, E-mail: christian.krell@tuwien.ac.at